Physics – Uspekhi **38** (11) 1271 – 1281 (1995)

INSTRUMENTS AND METHODS OF INVESTIGATION PACS numbers: 29.40.Wk; 79.20.Hx; 61.43.-j

Detectors of nuclear radiation and multiply charged particles with porous dielectric working media

M P Lorikyan†

Contents

Abstract. A review is given of the experimental investigations of the detection of radiation based on electron drift and multiplication in porous dielectrics subjected to an external electric field.

1. Introduction

The search for new particle detection and identification methods has been and remains one of the high-priority tasks in research. Physicists of our generation have witnessed the Wilson chamber being replaced with the bubble chamber, the development of the method of spark chambers, and the role played by the multiwire proportional chamber developed by Charpak. We have seen how the drive to increasingly high energies has exhausted the capabilities of Cherenkov radiation.' Then, the theoretical work of Ginzburg and Frank [1], Garibyan [2], Barsukov [2a], and Ter-Mikaelyan [3], who predicted the transition radiation, and the experimental studies of Yuan, Wang, and Prunster [4] and of Avakyan, Alikhanyan, Garibyan, Lorikyan, and Shikhlyarev [5], who were the first to discover x-ray transition radiation, have opened up new opportunities for developing methods suitable for measuring the energies of ultrarelativistic particles.‡ Methods based on semiconductor and gas microstrip detectors are developing rapidly at present.

Over the last 25 years the present author and his colleagues have been investigating electron drift and multi-plication in porous dielectrics under the influence of an external electric field. The use of a field makes it possible to investigate secondary electron emission in thick layers of porous dielectrics. This has led to the development of a series of new radiation detectors capable of detecting with 100% efficiency both strongly and minimally ionising charged particles, and also x-rays with a time resolution $\Delta t \leqslant 10^{-10}$ s and coordinate resolution $\Delta x \leqslant \pm 100$ μm. Another important feature of these detectors is the extremely small amount of matter in the path of a particle ($\sim 5 \times 10^{-4}$ g cm^{-2}).

This review is written in chronological order. It includes all the results that I know on particle detection based on electron drift and multiplication in porous dielectrics under the influence of an external electric field. I apologise for the omission of those results which I am not aware of and which are therefore not included in the review.

The need for this review has arisen because new important results have been obtained since the publication of the first review [9] and interest has now grown greatly in fast coordinate sensitive detectors containing a small amount of matter. The fullest information on standard secondary electron emission can be found in Ref. [10]. Some aspects of the results reviewed below are discussed also in Ref. [11].

2. Anomalous secondary electron emission

In 1936, Malter bombarded Al_2O_3 films, ~ 2000 A thick and deposited on metal substrates, with electrons of energies amounting to several hundreds of electron-volts. He discovered a secondary current which was up to 1000

† In Western literature the author's name is frequently spelled Lorikian.
‡ It was shown in Ref. [6] that x-ray transition radiation was not observed in earlier experiments [7, 8].

M P Lorikyan Erevan Physics Institute, ul. Brat'ev Alikhanyan 2, 375036 Erevan, Armenia. Fax (8-852) 35 00 39.
E-mail: intern@ird.erphy.armenia.su

Received 27 March 1995
Uspekhi Fizicheskikh Nauk **165** (11) 1323 – 1343 (1995)
Translated by A Tybulewicz

Table 1.

Material	BaO	Al_2O_3	MgO	LiF	KBr	CsI	KI	NaCl	CsBr
σ	1.05	1.3	3.8	~ 1	7.9	9.7	4.9	~ 8	–
λ/A	230	240	320	20	50	900	250	460	1200

times higher than the primary-electron current [12]. The secondary current rose slowly and reached its maximum after a certain time lag from the beginning of bombardment with the primary-electron beam. When this bombardment was stopped, the secondary current did not disappear immediately, i.e. delayed self-sustained emission was observed. Malter called this the *anomalous secondary electron emission* (ASEE). Further investigations [13–16] have shown that the Malter effect appears because of avalanche multiplication of electrons in a porous dielectric layer under the influence of an electric field of the positive charge that accumulates on the surface of a dielectric because of the loss of secondary electrons.

In 1966, Garwin and Edgecumbe [17] reported an investigation of secondary electron emission from porous KCl, $d = 15$ μm thick and with density $\rho = 3\%$ of the single-crystal density†, when a beam of electrons of $E_e = 100 - 1000$ MeV energy was transmitted by this emitter. The emitter was first bombarded with an intense electron beam of 10 keV energy. This beam passed through the KCl film and knocked out secondary electrons from its surface, so that the surface became positively charged. This charging beam was then removed and the emitter was bombarded with a high-energy electron beam. The average secondary emission coefficient was $\sigma \approx 5$ and it increased logarithmically with increase in E_e.

Soon after, Garwin and Llacer (18, 19] investigated ASEE of porous KCl(3.5%, 16) and CsI(3%) emitters when they transmitted single minimally ionising electrons. The method of creating an electric field was the same as that used by Garwin and Edgecumbe [17]. The results of this investigation were very disappointing since the value $\sigma \approx 1$ did not encourage interest in the Malter effect.

3. Mechanism of electron drift and multiplication in porous media

According to the model put forward by Jacobs [15, 16], a charged particle creates ionisation electrons in the pore walls and some of these electrons enter the pores, are accelerated by an electric field, and — having acquired a sufficient energy — knock out new electrons from the pore walls. This is repeated in all the generations of secondary electrons, so that all these electrons multiply in an avalanche-like manner inside a dielectric layer. Jacobs drew an analogy with a non-self-sustained discharge in a gas and expressed the secondary emission coefficient in the form

$$\sigma = \exp \alpha x, \tag{1}$$

where α is the number of secondary electrons formed by one avalanche electron per unit path length and x is the distance from the surface of a film to the point where a secondary electron is generated. A high value of σ is also a consequence of the high secondary electron coefficient of crystals of some alkali halide compounds and alkaline-earth oxides. Table 1 gives the values of σ for some materials obtained at primary electron energies 1–5 keV [10].

Good emission properties of these dielectrics are due to the large band gap ($\Delta W \approx 4 - 8$ eV) and are explained by the fact that in the slightly defective crystal lattice the internal secondary electrons of energy $W < \Delta W$ are in the conduction band and cannot lose energy by interacting with the valence-band electrons. (They lose energy mainly by the interaction with phonons.) Consequently, the energy lost by secondary electrons in dielectrics is low, the depth λ from which these electrons emerge is relatively high, and the majority of them reach the surface with a sufficient energy to overcome the surface barrier. The electron affinity χ (which is the difference between the electron energy at the bottom of the conduction band and in vacuum), which determines the energy of a potential barrier in these crystals, is small ($\leqslant 1$ eV), so that the emission of electrons into vacuum is quite considerable.

However, the technology of preparation of porous media used in the experiments reported in Refs [17–19] did not ensure the necessary cleanliness that would have prevented the adsorption of electronegative impurities and high-quality crystal structure of the pore walls. Therefore, these media had obviously a large number of bulk and surface defects. Irradiation of an emitter with a high-intensity beam of strongly ionising electrons for the purpose of charging the emitter surface creates a large number of electrons and holes inside the dielectric and these move in an electric field in opposite directions. If before the capture of electrons and holes by defects they manage to separate, a space charge appears in the dielectric and the electric field of this charge is directed opposite to the applied field. A space charge, on the one hand, weakens the field in the dielectric and prevents acceleration of secondary electrons and, on the other, it acts as a trap for these electrons and prevents their drift and multiplication.

4. Controllable secondary electron emission

Such highly simplified and qualitative considerations have led me to the conclusion that, if an external electric field is applied to a porous dielectric, a space charge will not appear inside it and instantaneous secondary electron emission with much higher values of σ can be expected [20].

Experimental investigations [21–25] have confirmed this conclusion. Investigations were made of secondary electron emission under the influence of an external electric field when a porous dielectric film transmitted a beam of 50 MeV electrons and the beam intensity was $\sim 10^8 - 10^9$ s^{-1}. Since the electron beam used in these experiments was of very high intensity and caused polarisation of the porous medium, the expected effect was not very clear. In the investigated emitters (Fig. 1) a film of a porous

† The density of a sample relative to the density of a single crystal (in percent) and the film or layer thickness (in microns) will be given directly after the chemical symbol for a porous material: for example, KCl(3%, 15).

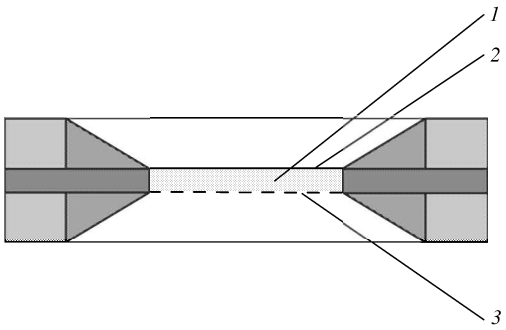

Figure 1. Section through an emitter of a controllable secondary electron emission detector: (*1*) porous material; (*2*) conducting substrate; (*3*) control grid.

material (*1*) was deposited on a thin conducting substrate (*2*). On the surface of this film or at a short distance from it there was a fine-mesh metal grid (*3*) with a high transparency (control grid). A potential V_g, positive relative to the substrate, was applied to the grid. Electrons formed in the porous film were extracted by the electric field through the openings in the grid, reached vacuum, and were collected by an anode.

The dependence of σ on the control grid potential obtained for an emitter made of porous KCl(2%, 100) had a region of slow rise, corresponding to the release of the ionisation electrons from the film without multiplication, and a region of steep rise where electron multiplication was observed in the pores.

When the grid was located on the surface of a porous KCl film, secondary electrons appeared immediately after the beginning of bombardment and the value of σ was the highest for a given V_g. An increase in the film thickness d shifted the $\sigma(V_g)$ curves towards lower values of V_g. However, when the grid was not located on the film surface, the dependence $\sigma(V_g)$ was still the same; but the maximum value of σ_{max} was not reached at the moment when bombardment was started, but much later. The rise time of σ increased with increase in the gap between the film surface and the grid. Hence, when the grid was not in contact with the film, the surface of the porous film became charged by the action of the transmitted beam. An analysis showed that these results were in agreement with the Jacobs model [15, 16] and the mean free path of the secondary electrons calculated on the basis of this model was $L_e \approx 1.3 \times 10^{-4}$ cm and it was independent of d.

Secondary electron emission from porous media under the influence of an external electric field was called the *controllable secondary electron emission* (CSEE).

The results reported in Refs [21–25] were confirmed by other authors [26] who described the results of an investigation of ASEE from porous CsI(4%, 125) irradiated with a high-intensity beam of 25 MeV electrons. The emitter used in this case did not have a control grid. The anode was located at a distance of 1.5 mm from the CsI film. Since the electron beam was of high intensity ($\sim 5 \times 10^{-9}$ A), it was capable of charging the film surface. All the characteristic properties of ASEE were reported, including for example, a time lag in the appearance of the secondary current and a low value of the secondary emission coefficient $\sigma_{max} \approx 5$.

An investigation reported in Ref. [27] and the subsequent experiments [28–31] demonstrated clearly the advantage of an external electric field when the intensity of the flux of particles crossing the emitter was so low that it did not cause polarisation effects. In these investigations we accelerated secondary electrons in a single-stage image converter with electrostatic focusing. The emitter in the CSEE detector (*2*) replaced the converter photocathode. The primary particles crossing this emitter were detected with a scintillation counter. Secondary electrons were accelerated to 14 keV and focused on the scintillation counter which contained an anthracene crystal calibrated for the number of secondary electrons n in a group ($n \leqslant 10^9$). The emitter was irradiated with β particles from a radioactive source and only those events were selected in which the ionisation created in the emitter by a β particle corresponded to the minimal ionisation.

The dependences of σ on the electric field E in KCl(2%) obtained for different values of d (Fig. 2) were of the same nature as in the case of irradiation with an electron beam [21–25], but σ_{max} was now considerably greater. This was why the $\sigma(E)$ curves were displaced towards lower values of E with increase in d, contrary to the results reported in Refs [21–25]. Hence, on the one hand, there was an increase in the number of the ionisation electrons and, on the other, the number of avalanche events increased in the film and a field of lower intensity was sufficient for the appearance of the same number of secondary electrons. When the film transmitted a beam, an increase in d increased the space charge, which suppressed electron drift and multiplication. Moreover, the presence of a control grid produced an inhomogeneous field in the film. When a beam was used, charging of the KCl surface opposite the grid cells resulted in equalisation of the field, so that the $\sigma(E)$ curves corresponded to regions with a lower field than the $\sigma(E)$ curves obtained for single particles when the effective value of E was considerably less. For $d = 180$ μm the control grid was located at 30 μm from the surface of the KCl film, but there was no emission time lag. This was due to the fact that in this case the emission of electrons occurred only under the influence of the external field.

The particle detection efficiency $\eta(E)$ increased with increase in E and reached a plateau at a level corresponding to the grid transparency of 70%. In fact, for a grid of 88% transparency the efficiency was $\eta = 0.87 \pm 0.2$ for films

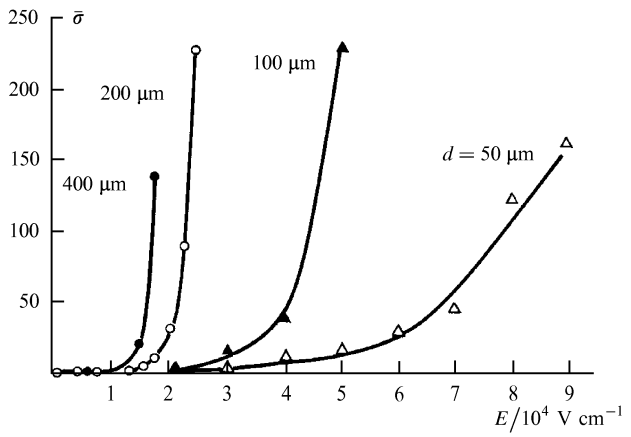

Figure 2. Dependences of the average value of the secondary emission coefficient $\bar{\sigma}$ on the electric field E, plotted for different thicknesses d of a porous KCl(2%) film.

$d = 300 - 400$ μm thick, but for $d = 50$ μm, it was $\eta = 0.59$ [28].

The number of secondary emission electrons observed in the $E = 0$ case was only $\sim 0.2 - 0.3$, according to the efficiency curves that took account of the grid transparency [27, 28], whereas in a film $d = 100$ μm thick about 100 electrons were formed. The number of electrons emitted under the influence of the field corresponding to the end of the linear part of the $\sigma(E)$ curve was approximately 8, i.e. only a small fraction of the ionisation electrons formed in the pore walls penetrated into the pores and participated in electron drift.

The fundamental question was the role of the substrate of porous dielectric films. It was found [32] that the emission at electron energies up to 15 keV was the same for a continuous conductor and for a grid. Hence, the KCl film covering the grid cells was sufficiently conducting. In the case of single particles the replacement of a continuous emitter substrate with a fine-mesh grid also did not change the dependences $\sigma(E)$ and $\eta(E)$. This was of practical importance, since it should make it possible to make particle detectors without a substrate and with the minimum amount of matter in the particle path.

The experimental distributions of the probability P_n of emission of n electrons from KCl(2%) of thickness d equal to 50, 100, 200, 300, and 400 μm were similar to those reported in Refs [18, 19] and had a maximum at $n \approx 0$. An increase in d or E increased the probability of emission of a large number of electrons. The distribution of P_n obtained for $E = 0$ was nearly of the Poisson type, but an increase in E increased the discrepancy between the results of measurements and the calculated Poisson distributions. Fig. 3 shows the distributions of P_n for $d = 400$ μm, determined at various values of V_g.

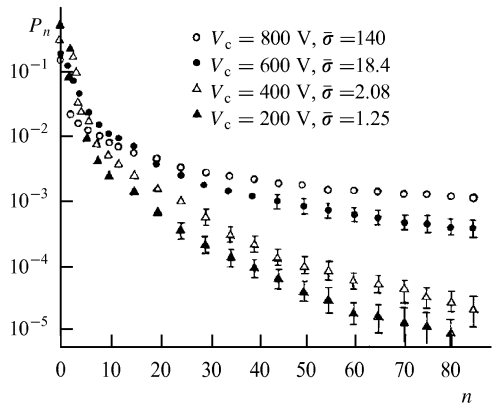

Figure 3. Statistical distributions of the numbers of emitted electrons, obtained for different values of V_g on irradiation of KCl(2%, 400) with β particles of $\geqslant 0.7$ MeV energy.

Investigations of the secondary-electron energy spectra were carried out using similar apparatus, but the emitter not only had a control grid, but also an additional grid subjected to a potential creating a retarding field. The electron energy was measured by the retarding field method. The energy spectra obtained for a film $d = 100$ μm thick, normalised to the maximum value in the distribution, are plotted in Fig. 4. For $E = 0$, the average energy of the electrons emerging from the emitter was $W_e = 2 \pm 1$ eV.

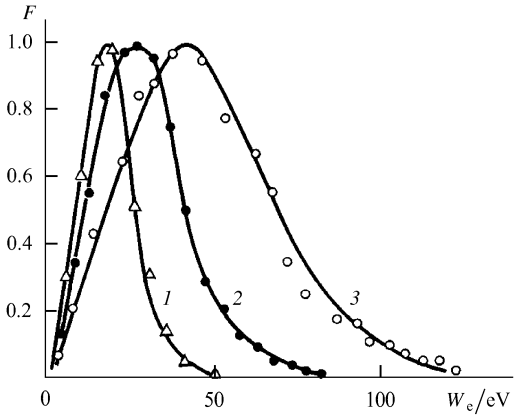

Figure 4. Energy spectra of emitted electrons obtained for $V_g = 2 \times 10^4$ V cm^{-1} (*1*), 3×10^4 V cm^{-1} (*2*), and 4×10^4 V cm^{-1} (*3*) by irradiation with β particles of > 0.7 MeV energy.

This result was in good agreement with the well-known data [10] and confirmed that, in the case of KCl, the electron affinity was $\chi \approx 2 \pm 1$ eV. The same conclusion was reached in Ref. [33] on the basis of an analysis of the results reported in Refs [17, 32, 34].

In determination of the mean free path L_e of secondary electrons we must bear in mind that, in contrast to primary particles which crossed the whole thickness of a porous film, the paths of secondary electrons can vary before they emerge from the emitter. Consequently, the number of multiplication cascades varies [29, 30], so that the observed emission is a superposition of avalanches and expression (1) should be replaced with

$$\sigma = \int_0^d \exp(\alpha x)\mathrm{d}x = \frac{(\exp)(\alpha d) - 1}{\alpha}. \tag{2}$$

According to Jacobs et al [16], we have

$$\alpha = A \exp \frac{1.64 U_i}{L_e E} \tag{3}$$

where $A = 10^3$ is a constant and U_i is the ionisation potential of the medium.

Table 2.

d/μm	50 ± 5	100 ± 5	200 ± 5	400 ± 5
L_e/μm	7.4 ± 0.7	9.9 ± 0.5	8.4 ± 0.4	11.0 ± 1.5

The results of measurements are in good agreement with this model, as demonstrated by the good fit of the experimental points to a linear dependence of ln σ on E. The values of L_e predicted by this model for KCl(2%) and $U_i = 10$ eV are listed in Table 2. The average value of L_e can also be determined from the energy spectra of secondary electrons on the assumption that the energy spectrum of those secondary electrons which leave the surface of the dielectric is similar to the energy spectrum of the electrons inside the film [15, 16]. We then have

$$L_e = 10.66 \frac{W_e}{\pi^2} eE, \tag{4}$$

where W_e is the average energy of secondary electrons. Calculations based on expression (4), in combination with the known energy spectrum of secondary electrons, give $L_e = 10 \pm 1.5$ μm for KCl(2%, 100).

5. Porous emission detectors

The ionisation density for multiply charged ions and fission fragments is considerably higher than for a particle causing minimal ionisation and, therefore, their ranges in matter are small and they are difficult to detect. If a CSEE detector is used, these difficulties are partly avoided because, first, the source and the detector can be placed inside the same vacuum chamber, and, second, the low density of the working medium means that heavy particles penetrate deeper into this medium and create less ionisation per 1 cm of the path than in a dense medium.

Lorikyan and Trofimchuk developed porous emission detectors and investigated their operation when they were irradiated with α particles of ~ 4 MeV energy [35, 36]. The porous film substrate was made of Al_2O_3, 1 μm thick [37], coated by an Al film ~ 0.1 μm thick. A control grid of 70% transparency was located on the surface of a KCl(2%, 100) porous film. The ionising capacity of these α particles was over 10^9 times greater than that of β particles, so that unsurprisingly their distributions were quite different and their maxima corresponded to $n_p \gg 1$. These distributions are plotted in Fig. 5 for different values of V_g. The relative half-width at half-amplitude of the distribution of $\Delta n/n_p$ began to decrease with increase in V_g, but from the onset of the avalanche processes it started to rise again (Table 3). The minimum value of $\Delta n/n_p$ corresponded, as expected, to V_g at which the dependence $n(V_g)$ became nonlinear, i.e. it corresponded to the maximum collection of the ionisation electrons. When electron multiplication predominated, the fluctuations of n, which were now mainly due to this process, became stronger.

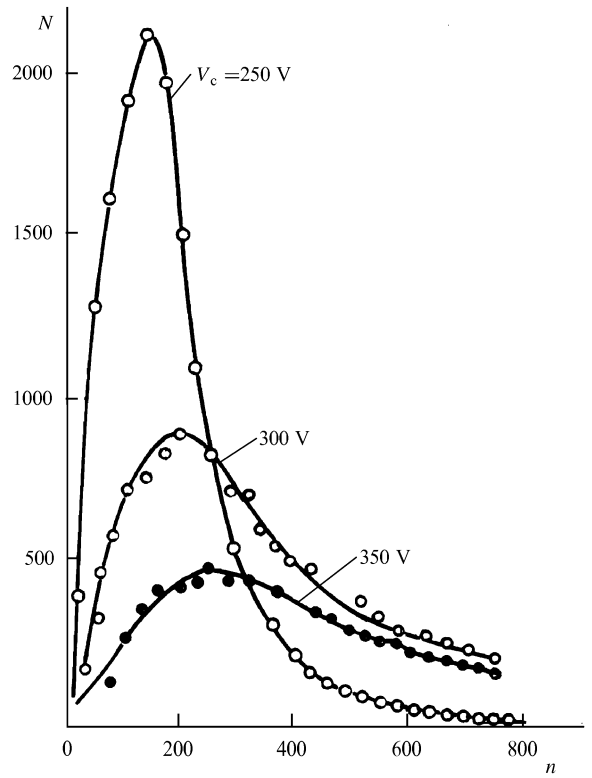

Figure 5. Statistical distributions of the numbers of electrons emitted by the passage of α particles of ~ 4 MeV energy, determined for various values of V_g.

Table 3.

V_g/V	0	100	150	200	250	300	350	400
$\Delta n/n_p$	4	2.5	2.25	1.8	1.1	1.5	2.2	4.0

With the exception when $V_g = 0$, corresponding $\sigma(\alpha) \approx 3$, the nature of the secondary emission induced by α particles (Fig. 6) was practically the same as that produced by β particles (Fig. 2). In all cases the value of σ_{max} corresponded to the prebreakdown value of V_g. Since the ionising ability of the α particles was approximately 10^9 times greater than that of the β particles and in view of the results plotted in Figs 2 and 6, it was reasonable to conclude that an increase in the ionisation density did not increase linearly the effective value of n, i.e. the ionisation electrons were captured by ions formed by the α particles themselves. An increase in E caused, as in the previous cases, the value of n_p to rise slowly and then to increase steeply. The maximum efficiency of detection of α particles was $\eta = 100\%$. The time dispersion of porous emission detectors, calculated taking account of the contribution of the rest of the apparatus, was close to 0.75×10^{-9} s. It was concluded that the true dispersion, caused by electron drift and multiplication in the porous medium, was considerably less than 10^{-9} s.

The feasibility of detecting strongly ionising particles against the background of weakly ionising radiation was

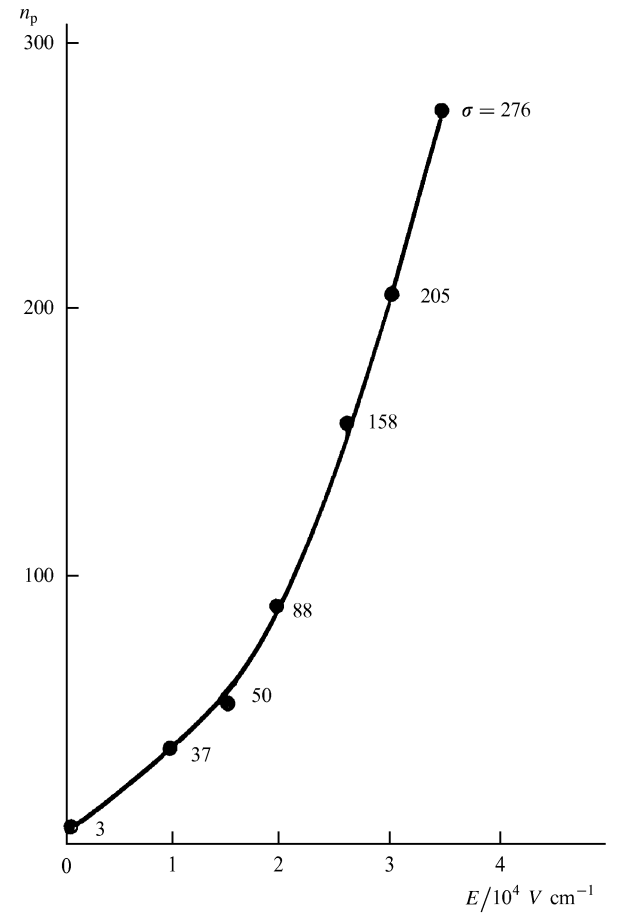

Figure 6. Dependence of the probable number of electrons emitted as a result of a passage of an α particle on the electric field E, obtained for KCl(2%, 100).

Table 4.

Lowest electron-detection-threshold/mV		10	50	100	200
η (%)	α particles	99.4	99.0	97.6	95
	β particles	7	2	—	—

also investigated [38]. The detector was similar to that described in Ref. [35] but the α-particle source was located in the vacuum part of the detector and the working substance was MgO(0.7%, 100). The α-particle energy was 5.5 MeV. In the case of α particles the value of n_p exceeded 2000, but for β particles it was approximately 20. The results (Table 4) indicated that selection of the lower threshold of detection of the secondary electrons could exclude the particles causing minimal ionisation and yet retain the efficiency of detection of the strongly ionising radiation at the level of 100%.

A promising working medium for porous detectors is cryolite (Na_3AlF_6). It has good emission properties, is not hygroscopic, and is used to fabricate strong and stably operating emitters for porous detectors characterised by $\sigma_{max} \approx 4000$ for α particles (Fig. 7). An investigation of CSEE emitters made of KBr, LiF, and MgU was also made [39] and the results are given in Fig. 8.

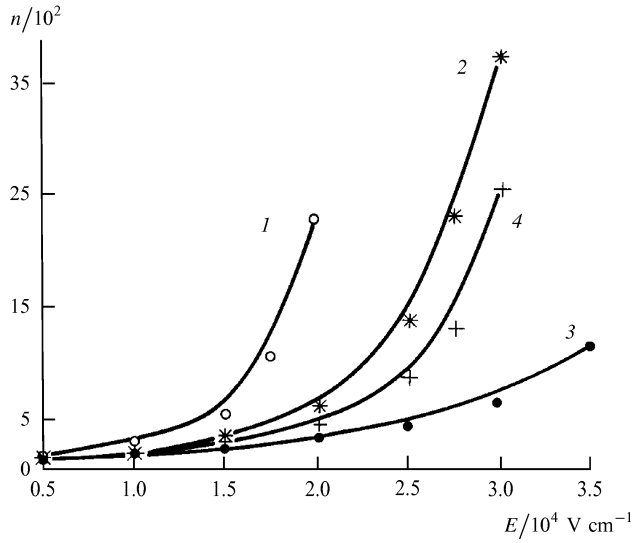

Figure 7. Dependence, on E, of the average number of electrons emitted as a result of passage of an α particle, obtained for cryolite (1%) emitters of different thicknesses d (μm): (*1*) 300; (*2*) 200; (*3*) 100; (*4*) 200. Curve *4* was obtained when the substrate of the porous emitter was a fine-mesh grid with cells of 80 μm × 80 μm size [39].

The high effective atomic numbers of KBr, CsI, cryolite, etc. means that x-ray photons can also be recorded efficiently [39].

The system for recording secondary electrons in porous emission detectors should have a high gain, good time parameters, and be subject to just small statistical fluctuations of the gain. This was ensured by the use of microchannel plates [40, 41]. In one detector a chevron configuration of two microchannel plates was located directly in front of the emitter.

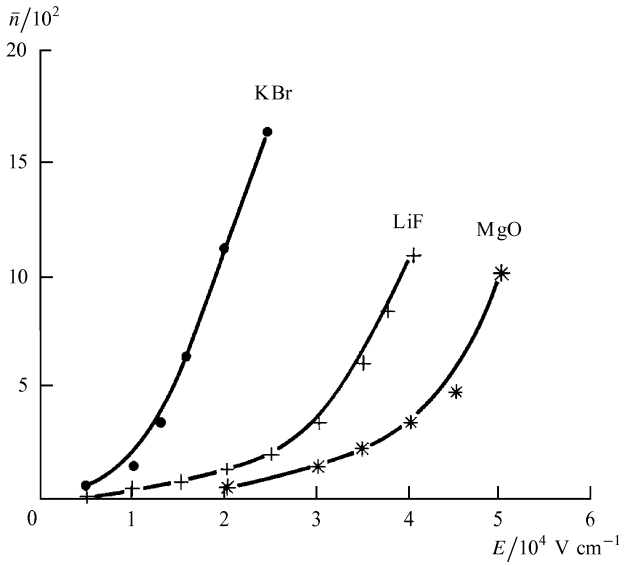

Figure 8. Dependence, on E, of the average number of electrons emitted as a result of the passage of an α particle, obtained for KBr (1%, 100), LiF (1%, 100), and MgO (0.9%, 100).

In another CSEE detector the emitter replaced a photomultiplier photocathode and a chevron configuration of two microchannel plates replaced the first dynode. In this case the α particles crossed the emitter without reaching the microchannel plates. The efficiency of detection of the 5.5-MeV α particles increased with increase in V_g and reached a plateau at $\eta = 100\%$ in the case of both MgO(1%, 100) and KBr(1%, 100). The time resolution of this detector was approximately 0.5 ns.

Isochronous transport of secondary electrons by en electrostatic mirror was also found to be very promising [51]. A detector of this type with MgO(0.6%, 100) as the working substance was described in Refs [42–44]. A fine-mesh nickel grid, covered by a thin metallised colloid film, supported MgO. A control grid was located at 0.5 mm from the surface of the MgO film. Secondary electrons were detected by two microchannel plates with a coaxial anode. The time resolution of two such synchronously working detectors was 0.25×10^{-9} s and the efficiency of detection of 4.5–7.5 MeV α particles was 100%. The spectrum of the α particles from the ^{226}Ra sources, determined by the investigators, led them to the conclusion that the CSEE detectors could be used successfully in nuclear spectroscopy.

A time-of-flight spectrometer for heavy ions, containing two CSEE detectors, with synchronous electron transport was described in Ref. [44]. The time resolution of the spectrometer was 0.12 ns and it was used in diagnostics of 115 MeV ^{132}Xe ions.

The phenomenon of CSEE was investigated and used to detect various particles in a study reported in Ref. [45]. Secondary electrons were accelerated by a field of 14 kV cm^{-1} intensity and detected with a semiconductor detector. Electron drift in a porous medium occurred under the influence of the same field. In 2 h after application of the voltage the value of σ for porous CsI fell from 15 to 3 for β particles and from 2000 to 100 for α particles; this value then remained constant. Such changes were not observed for KCl. The emission properties were restored by the application of a reverse depolarising electric field, in a manner similar to that described in Refs [53–57]. It was

found that stable emission was observed when the condition $E_d t_d > E t_w$ was obeyed; here, E_d and t_d are the intensity and duration of application of the depolarising field and t_w is the duration of application of the working voltage. The porous emission detector described in Ref. [45] was subjected to an alternating voltage in order to avoid the polarisation effects in the working medium. This voltage was applied by an additional thin electrode located at 1 cm from the surface of the porous CsI film. The electrode was covered by a dense CsI film which was 600 A thick. The electrons emerging from the porous film were accelerated in the gap between the additional electrode and the porous emitter to an energy of 5.5 keV and were then multiplied in the dense CsI film by a factor of 6–7. Next, they were accelerated again by the field of 14 kV cm^{-1} and were focused on an assembly of two microchannel plates. The time resolution of the detector was 600 ps and the efficiency of detection of minimum-ionisation β particles was $\eta = 92\%$. This detector was used in a time-of-flight system to detect protons of 540 MeV energy. The alternating voltage applied to the detector was synchronised with the time structure of the proton accelerator. The efficiency of proton detection was 96% –98% and the time resolution of the detector was 450 ps, which was considerably better than in the case of β particles. This result was attributed in Ref. [45] to the higher [by a factor of 1.5] ionisation energy losses suffered by protons, compared with those for β particles, and the consequent result of smaller time fluctuations.

In the case of porous KCl emitters it was found [45] that there were some contradictions between the results obtained and those reported in Refs [53–57], where a fall of the particle detection efficiency with time was observed. However, these contradictions could be explained by the considerably higher field intensity used in Refs [53–57]. On the other hand, it was reported in Refs [27–31], in which cases the field intensity was comparable with that of the fields applied to KCl, CsBr, MgO, and LiF [45], that no changes in σ with time were found when a depolarising field was not used.

A CSEE detector in which the control grid was replaced with a continuous anode was investigated [46]. In this detector the anode was located on the surface of a porous CsI(1%) film and the signals were amplified, as in Refs [53–57], by a wide-band amplifier. The authors of Ref. [46] found that the amplitude resolution of the detector improved with increase in V_g and reached 15%.

The technology used in the preparation of porous films has a strong influence on their emission properties [39]. It was found that if after a preliminary heating of Mg a boat from which evaporation took place was not heated any further, i.e. if MgO was deposited only as a result of self-heating of Mg, the porous films were transparent and had poor emission characteristics. However, when the boat was heated continuously throughout the deposition of MgO, the films were of white matt colour and contained MgO microcrystallites of 10–15 μm size. The emitters then had high values of σ, operated more stably, and the fluctuations of σ were much less. The thickness of MgO was a linear function of the pressure of air in which the deposition took place. A strong reduction in this pressure caused deterioration of the emitter quality. After contact with air, the properties of porous KBr films changed greatly. The thickness of the films decreased, they became mechanically stronger, but their emission properties were much worse. Films of LiF and MgO were not affected by moisture, whereas those of CsI were moderately hygroscopic.

6. Statistics of controllable secondary electron emission

Kharitonov [48] considered theoretically the problems of the statistics of electron drift and multiplication in porous media subjected to an external electric field. He adopted an analogy with the problem of fluctuations of the gain due to the gas in proportional counters. At the time of publication of Kharitonov's contribution the statistics of CSEE had not yet been investigated experimentally and, therefore, the model could not have been checked quantitatively. The model was compared with the experimental results by Gavalyan [49].

The experimental results reported in Ref. [49] for Na_3AlF_6(1%, 200) and the calculated distributions are compared in Fig. 9.

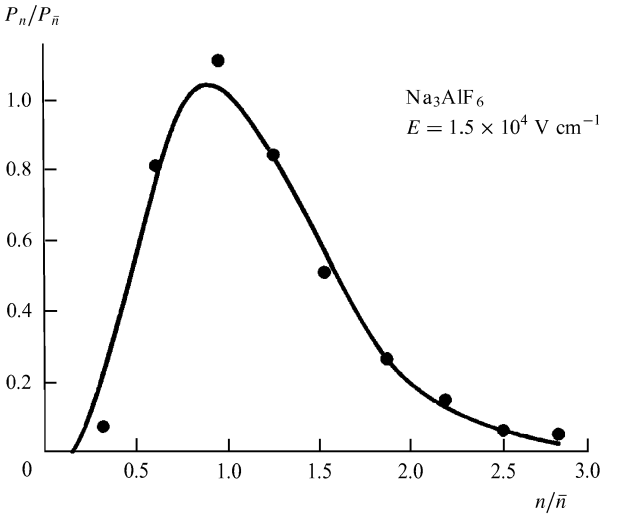

Figure 9. Distribution of the probability P_n of the emission of n electrons by the action of α particles on Na_3AlF_6(1%, 200). The points are the experimental values and the continuous curves are calculated. $E = 1.5 \times 10^4$ V cm^{-1}.

Electron multiplication in porous media was considered in Ref. [50] on the basis of a model of signal amplification in a channel multiplier. A comparison was made there of the statistical distributions obtained on the basis of this model with the authors' own experimental data for MgO(0.4%, 100) and agreement was reported. The agreement of the experimental results with both theoretical models would suggest that, on the one hand, a porous medium resembles a gas because of the random distribution of the pore sizes and, on the other, since the multiplication processes occur in discrete pores, such a medium has properties resembling those of channel multipliers.

7. Multiwire porous detector

None of the radiation detectors listed above had been used to measure the particle coordinates, although this is possible. For example, if the photocathode of a multistage

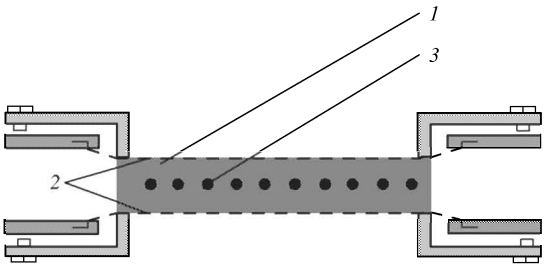

Figure 10. Section through a multiwire porous detector: (*1*) porous material; (*2*) cathodes; (*3*) elementary anodes.

image converter is replaced with a CSEE emitter, the coordinates of a particle can be determined from the converter screen.

A multiwire porous detector, similar to a multiwire proportional chamber but with a gas replaced by a porous dielectric, is promising (Fig. 10). Cathodes (*2*) made of a fine-mesh grid, are parallel to one another. Between them, separated by distances L from each cathode, there are stretched anode filaments (*3*) of radius r_0 and arranged in steps of l. The space between the cathodes is filled with a porous dielectric (*1*).

Let us estimate the number of electrons M, collected by an anode of such a multiwire porous detector as a result of passage of minimally ionising particles, on the basis of the known dependence $\sigma(E)$ (Fig. 2). Let us split the whole thickness of the working film of the detector into elementary layers, each of thickness L_e. Then, $M = \prod_{i=1}^{k} \delta(E_i)$, where E_i and $\delta(E_i)$ are the electric field and the emission coefficient of the ith layer, respectively, and k is the number of such elementary layers. Since the electric field has a near-cylindrical geometry, we have $E_i \approx (U_w/r_i)\ln(L/r_0)$, where U_w is the difference between the cathode and anode potentials (working voltage), r_i is the distance from the centre of an anode filament to the centre of the ith layer, L is the distance between the anode and the cathode, and r_0 is the radius of an anode filament. We can determine $\delta(E_i)$ by dealing with a CSEE emitter in a similar manner, splitting it into elementary layers of thickness L_e. Since the electric field is then homogeneous the values of δ_i are the same for all the layers, so that we have $\sigma(E_i) = \delta^k(E_i)$. Hence, substitution of $\delta(E_i)$ in the expression for M gives $M = \prod_{i=1}^{k} \sqrt[k]{\sigma(E_i)}$. In the case of a multiwire porous detector filled with KCl (2%, $L_e = 10$ μm), $L = 300$ μm, $r_0 = 10$ μm, and $U_w = 1.5 \times 10^9$ V and calculations give $M \approx 6 \times 10^4$.

In the subsequent experiments [53–57] the signals were amplified with a wide-band amplifier characterised by the gain of about 200. It was established that the gain in a multiwire porous detector filled with porous MgO oscillated strongly and decreased during operation. In the case of KCl and CsI there were no such gain oscillations, but the particle detection efficiency fell with time by an amount which was greater for larger initial values of the gain.

The values of η for CsI and KCl decreased even in the absence of radiation, but this was a slower process than during irradiation. The results for CsI(2%) obtained during continuous irradiation and when the α-particle source was operating only for 2–3 s during measurements are compared in Fig. 11. In the case of CsI the working

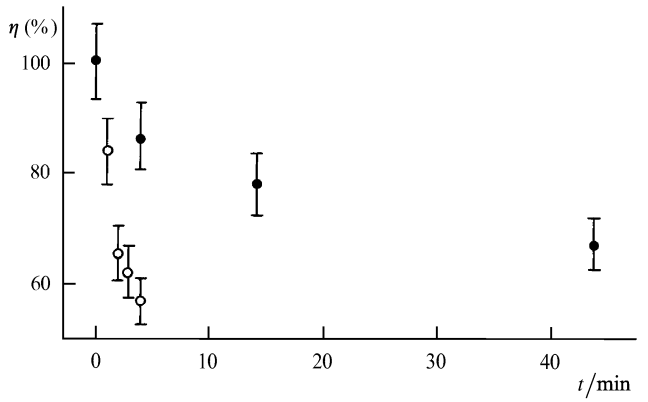

Figure 11. Decay of the detection ability of α particles by a multiwire porous detector based on CsI (2%): the open circles represent continuous irradiation and the black dots correspond to the case when the detector was not irradiated between the measurements.

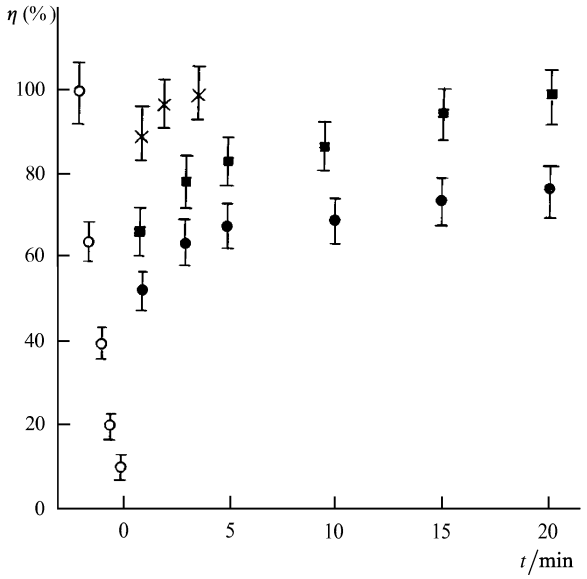

Figire 12. Recovery of the efficiency of detection of α particles by a multiwire porous detector based on CsI (2%): the open circles show the decay with time and the black dots represent the spontaneous recovery when the power supply was switched; the squares and the crosses correspond to recovery under the action of a depolarising voltage $U_d = 300$ V or $U_d = 600$ V, respectively.

characteristics of a multiwire porous detector were restored even after a steep fall, provided the working voltage U_w was switched off for a time. The circles in Fig. 12 were obtained for continuous operation of the detector and the dots for the case when, after the fall of η, a pulsed voltage was applied only during measurements. When after the fall of η the detector was subjected for a time t_d to a depolarising voltage U_d opposite to U_w, the recovery of η was much faster in the case of the KCl and CsI emitters. The results are plotted in Fig. 13 for $U_d = 300$ V and $U_d = 600$ V, respectively. In the case of MgO such a depolarising voltage did not restore the efficiency but caused weak breakdowns in the emitter.

It is not easy to interpret these results because of the extreme complexity of the structure of porous media, the uncontrolled amounts and nature of the impurities, and the nature of the crystal structure of the pore walls.

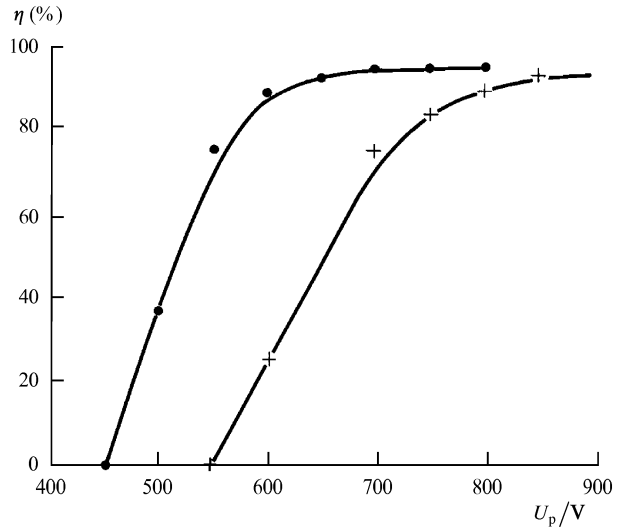

Figure 13. Dependence of the efficiency of detection of α particles on the amplitude of the working voltage pulses U_w, obtained for chemically pure CsI (1.0%) when the depolarising voltage was $U_d = 300$ V (points) and for CsI (2%) and $U_d = 600$ V (crosses); $t_w = 2$ ms and $t_d = 18$ ms.

The slow fatigue effect observed for multiwire porous detectors in the absence of any ionising radiation could be explained qualitatively by the appearance of an ion current in a dielectric in accordance with the Frenkel mechanism [58]. As a result of thermal fluctuations, some of the ions in a dielectric acquire an energy sufficient for migration and reach interstices. An electric field sets these ions in directional motion. Some of the ions may be captured by traps, resulting in the accumulation of a positive charge. On the one hand, the field of such a space charge weakens the external field and, on the other, it acts as a trap for electrons drifting towards the anode. Spontaneous recovery of the operational capability of a multiwire porous detector occurs under the influence of an internal residual space-charge field, which restores ions to their previous state, so that equilibrium is recovered in the working medium.

Electrons and holes participate in the process when a detector is bombarded with ionising radiation. Since amplification occurs in a small region around anode filaments, the carrier density in the space near the anodes is high and, therefore, the polarisation phenomena become important.

A multiwire porous detector operates stably when the working and depolarising voltages are applied alternately in the form of pulses and the durations and amplitudes of these pulses are in certain ratios. These ratios depend on the nature of the working medium, its density and thickness, and also on the internal gain of the detector. In particular, in the case of KCl multiwire porous detectors, (2%, $L = 200$ μm, $l = 250$ μm, $r_0 = 12.5$ μm with $U_w = 850$ V, $t_w = 10$s, $t_d = 1$ s) the detection of α particles with 100% efficiency and stable operation of the detector are attainable for $U_d = 550$ V.

In the millisecond range of the values of t_w and t_d the stability conditions are essentially similar [59]. Table 5 gives the results of measurements of the stability of the efficiency η over a period of 30 min in the region of the plateau of the efficiency curve for α particles when chemically pure CsI was used and the multiwire porous detector parameters

Table 5.

t_w/ms	t_d/ms	η_{max}(%)		$\Delta\eta$ (%)	
		$\delta/\delta_0 = 1\%$	$\delta/\delta_0 = 2\%$	$\delta/\delta_0 = 1\%$	$\delta/\delta_0 = 2\%$
1	19	97	100	0 ± 0.025	0
2	18	93	92	0 ± 0.03	0 ± 0.036
3	17	92	81	0 ± 0.024	0 ± 0.042
4	16	91	74	0 ± 0.025	0.3 ± 0.06
5	15	88	—	0 ± 0.026	0.3 ± 0.06

were $L = 280$ μm and $l = 500$ μm. The first and second columns of Table 5 give the values of t_w and t_d, the third and fourth columns give η_{max} at the beginning of operation for the emitter densities 1% and 2%, respectively, and the fifth and sixth columns illustrate the fall of η for $U_d = 500$ V and CsI(1%) and for $U_d = 600$ V and CsI(2%).

The $\eta(U_w)$ curves for a multiwire porous detector containing chemically pure CsI(1%) and CsI(2%) with $L = 280$ μm and $l = 500$ μm are plotted in Fig. 13. In the case of technically pure CsI these curves are similar, but U_w is $\sim 50\%$ higher [59]. Under these conditions it is possible to detect minimally ionising particles by applying a voltage U_w which is twice as high; the value $\eta = 100\%$ is reached at higher L than in the case of α particles [60]. Investigations [39] have demonstrated that cryolite also becomes polarised during operation, but this can be corrected effectively by a depolarising voltage, which is not true of KBr. The dependences $\eta(U_w)$ for cryolite(1%), CsI(1.5%), and KBr(1%) obtained for α particles reaching a multiwire porous detector with $L = 200$ μm and $l = 500$ μm are plotted in Fig. 14.

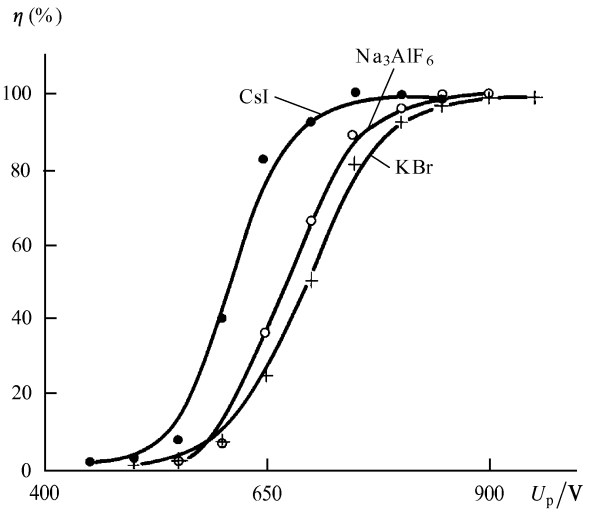

Figure 14. Dependence of the efficiency of detection of α particles on the amplitude of the working pulses U_w, obtained for a multiwire porous detector based on CsI (1.5%), KBr (1.0%), or cryolite (1.0%) with $L = 200$ μm and $l = 500$ μm.

An emission variant of a multiwire porous detector has anode filaments outside the working medium and electrons are collected after emission into vacuum. The dependence $\eta(U_w)$ for such emission detectors is of the same form as that for multiwire porous detectors, but the working voltage is considerably higher [61–63].

Multiwire porous detectors can be used successfully also in detection of low-energy x-ray photons against the background of hard γ rays, because of a large selection of porous emitters with different atomic numbers, densities, and thicknesses of the working substance. A multiwire porous detector containing CsI and KBr ($L = 2$ mm, $l = 250$ μm) was used [64] to detect Mossbauer x-ray photons of energy $E_\gamma = 6$ keV against the background of photons with $E_\gamma = 6$ keV and $E_\gamma = 120$ keV, since $\eta = 80\%$ for $E_\gamma = 14$ keV and $\eta \approx 6\%$ for $E_\gamma = 120$ keV.

It was concluded in Ref. [64] that multiwire porous detectors based on KBr gave better results for x-ray photons with $E_\gamma = 6$ keV than a scintillation counter with a CsI : Tl crystal.

The absolute value of η for 6 keV photons was determined [65] with a multiwire porous detector calibrated against a semiconductor detector. Fig. 15 gives the $\eta(U_w)$ curves obtained for a multiwire porous detector with CsI(2%), characterised by $L = 400$ μm and $l = 250$ μm, and bombarded with γ photons ($E_\gamma = 5.9$ keV) and β particles.

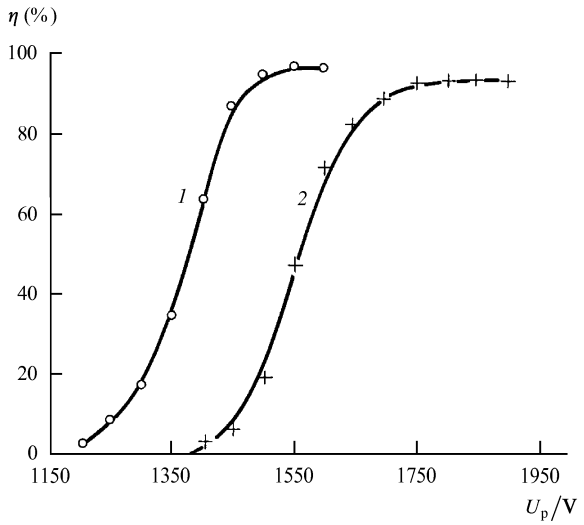

Figure 15. Dependences of the efficiency of detection of β particles of > 0.7 MeV energy (*2*) and of x-ray photons of 5.9 keV energy (*1*) by a multiwire porous detector based on CsI (2%) with $L = 400$ μm and $l = 250$ μm.

8. Microstrip porous detector

The working area of a multiwire porous detector is limited by the difficulties associated with the need to stretch anode wires separated by distances of the order of 0.1 mm from one another. This problem is avoided in microstrip detectors and the difficulties associated with the large cathode area are solved by metallisation of the surface of a porous dielectric. A microstrip detector which I developed [70] has the working substance CsI (1% – 2%) and strips 100 μm wide separated by gaps of 100 μm and with a porous layer 500 μm thick. The detector was investigated by irradiation with α particles. The number of readings per unit time increased with increase in U_w and reached a plateau ($\eta = 100\%$).

9. Time, amplitude, and coordinate resolution of multiwire porous detectors

The strong absorption of the ionisation electrons by the pore walls results in very strong fluctuations of the number of electrons reaching the pores, so that it is not possible to use multiwire porous detectors in high-precision measurements of the ionising capability of particles. The best amplitude resolution of 25% for irradiation with α particles was reported in Refs [67, 68] when the signals were recorded separately from each wire in a multiwire porous detector. However, the time resolution of this detector was exceptionally high. This was due to the fact that the average energy of the internal electrons was relatively high (~50 eV) and, therefore, the avalanche formation time was short. According to Refs [67 and 68], the time resolution of a multiwire porous detector was 60 ps or less.

The coordinate resolution of a multiwire porous detector reported in Ref. [57] was ±100 μm or less. The high position resolution was achieved not only because the pore diameters were small, but because the pores were close, i.e. branching of the flux of the drifting electrons and the motion away of the core of an electron avalanche were prevented. The fact that the pores were closed was indicated by the dependence of the secondary electron emission coefficient σ on the density of the porous medium (see Fig. 13). In fact, the same values of σ corresponded to the same energies of internal electrons $W_e = eEL_e$, where L_e is proportional to the pore radius r which in its turn is proportional to $\rho^{-1/3}$ or $\rho^{-1/2}$ for spherical or cylindrical pores, respectively (ρ is the density of the medium). The experimental results indicated that $\sigma \propto \rho^{-1/3}$.

10. Conclusions

The effective electron drift and multiplication in porous dielectrics under the action of an external electric field, discovered over 25 years ago, provides unique opportunities for the construction of fast, coordinate-sensitive, inexpensive detectors of nuclear radiation and multiply charged ions with a very small amount of matter in the path of the particles. This effect can also be used in other branches of technology, such as electron multipliers, image converters, and possibly also in television technology.

Acknowledgements. I wish to acknowledge the major role of N N Trofimchuk and V G Gavalyan in the development of the detector technique based on porous dielectrics, and to thank V G Gavalyan and A S Esin for their help in preparation of this review, and also G I Merzon for valuable advice given in discussing the review.

References

1. Ginsburg V L, Frank I M *J. Phys. USSR* **9** 353 (1945)
2. Garibyan G M *Zh. Eksp. Teor. Fiz.* **37** 527 (1959) [*Sov. Phys. JETP* **10** 372 (1960)];
   (a) Barsukov K A *Zh. Eksp. Teor. Fiz.* **37** 1106 (1959) [*Sov. Phys. JETP* **10** 787 (1960)]
3. Ter-Mikaelyan L M *Dokl. Akad. Nauk SSSR* **134** 318 (1960) [*Sov. Phys. Dokl.* **5** 1015 (1961)]
4. Yuan L C L, Wang C L, Prunster S S *Phys. Rev. Lett.* **23** 496 (1969)

5. Avakyan K M, Alikhanyan A I, Garibyan G M, et al. *Izv. Akad. Nauk ArmSSR Fiz.* **5** 267 (1970); Alikhanian A I, Avakian K M, Garibian G M, et al. *Phys. Rev. Lett.* **25** 635 (1970)
6. Lorikyan M P, Sardaryan R A, Shikhlyarov K K *Izv. Akad. Nauk Arm. SSR Fiz.* **24** (4) 159 (1989); **24** (5) 151 (1989); **24** (6) 300 (1989)
7. Arutyunyan F R, Ispiryan K A, Oganesyan A G *Izv. Akad. Nauk SSR Ser. Fiz.* **28** 1864 (1964); *Yad. Fiz.* **1** 842 (1965) [*Sov. J. Nucl. Phys.* **1** 604 (1965)]
8. Arutyunyan F R, Ispiryan K A, Oganesyan A G *Pis'ma Zh. Eksp. Teor. Fiz.* **4** 277 (1966) [*JETP Lett.* **4** 187 (1966)]
9. Lorikyan M P *Tr. II Simpoziuma po Perekhodnomu Izlucheniyu Chastits Vysokikh Energii, Erevan, 1983* (Proceedings of Second Symposium on Transition Radiation of High-Energy Particles, Erevan, 1983) (Erevan: Erevan Physics Institute, 1984) p. 657
10. Bronshtein I M, Freiman P S *Vtorichnaya Elektronnaya Emissiya* (Secondary Electron Emission) (Moscow: Nauka, 1969)
11. Bolozdynya L M *Prib. Tekh. Eksp.* (2) 5 (1984)
12. Malter L *Phys. Rev.* **50** 48 (1936)
13. Zernov D V *Zh. Eksp. Teor. Fiz.* **17** 1787 (1937); *Dokl. Akad. Nauk SSSR* **8** 352 (1944)
14. Sternglass E J, Goetze G W *IRE Trans. Nucl. Sci.* **NS-8** 3 (1962); **NS-9** 97 (1962)
15. Jacobs H *Phys. Rev.* **84** 877 (1951)
16. Jacobs H, Freely J, Brand F A *Phys. Rev.* **88** 492 (1952)
17. Garwin E L, Edgecumbe J, Preprint SLAC-PUB 156 (1965)
18. Garwin E L, Llacer J, Preprint SLAC-PUB 623 (1969); *J. Appl. Phys.* **41** 1489 (1970)
19. Llacer J, Garwin E L *J. Appl. Phys.* **40** 101 (1969)
20. Lorikyan M P, Doctoral Thesis in Physicomathematical Sciences (Dubna: Joint Institute of Nuclear Research, 1975)
21. Lorikyan M P, Kavalov R L, Trofimchuk N N, Davtyan E E *Izv. Akad. Nauk Arm. SSR Fiz.* **6** 297 (1971)
22. Lorikyan M P, Kavalov R L, Trofimchuk N N, Serov V L *Izv. Akad. Nauk ArmSSR Fiz.* **7** 18 (1972)
23. Lorikyan M P, Kavalov R L, Trofimchuk N N *Izv. Akad. Nauk Arm. SSR Fiz.* **8** 33 (1973)
24. Lorikyan M P, Kavalov R L, Trofimchuk N N *Pis'ma Zh. Eksp. Teor. Fiz.* **16** 320 (1972) [*JETP Lett.* **16** 226 (1972)]
25. Lorikyan M P, Kavalov R L, Trofimchuk N N *Nauchn. Soobshch. Erevan. Fiz. Inst.* (19) (1973)
26. Cheehab R, Humbert G, Leblond B, Preprint LAT/RT/83-13 (Orsay, France: 1983)
27. Lorikian M P, Kavalov R L, Trofimchuk N N, Preprint EFI-40(73) (Erevan: 1973); *Nucl. Instrum. Methods* **122** 377 (1974)
28. Lorikyan M P, Kavalov R L, Trofimchuk N N, Arvanov A N *Nauchn. Soobshch. Erevan. Fiz. Inst.* (84) (1974)
29. Lorikyan M P, Kavalov R L, Trofimchuk N N, et al. *Nauchn. Soobshch. Erevan. Fiz. Inst.* (131) (1975)
30. Trofimchuk N N, Lorikyan M P, Kavalov R L, et al. *Zh. Eksp. Teor. Fiz.* **69** 639 (1975) [*Sov. Phys. JETP* **42** 324 (1975)]
31. Arvanov A N, Kavalov R L, Lorikyan M P, Trofimchuk N N *Izv. Akad. Nauk Arm. SSR Fiz.* **9** 540 (1974)
32. Lorikyan M P, Kavalov R L, Trofimchuk N N *Radiotekh. Elektron.* **14** 935 (1969)
33. Lorikyan M P, Knyazyan S G *Izv. Akad. Nauk Arm. SSR Fiz.* **5** 180 (1970)
34. Kavalov R L, Lorikyan M P, Trofimchuk N N *Izv. Akad. Nauk Arm. SSR Fiz.* **3** 63 (1968)
35. Lorikyan M P, Trofimchuk N N, Preprint EFI-178(24) (Erevan: 1976); *Nucl. Instrum. Methods* **140** 505 (1977)
36. Lorikyan M P, Trofimchuk N N *Tr. Mezhdunar, Simpoziuma po Perekhodnomu Izlucheniyu Chastits Vysokikh Energii, Erevan, 1977* (Proceedings of International Symposium on Transition Radiation of High-Energy Particles) (Erevan: Erevan Physics Institute, 1978) p. 449
37. Kavalov R L, Lorikyan M P, Trofimchuk N N *Izv. Akad. Nauk Arm. SSR Fiz.* **2** 443 (1967)
38. Arvanov A N, Akhperdzhanyan A G, Gavalyan V G, et al. *Prib. Tekh. Eksp.* (4) 58 (1981)
39. Gavalyan V G, Arvanov A N, Gukasyan S M, Lorikyan M P *Izv. Akad. Nauk Arm. SSR Fiz.* **19** 152 (1984)
40. Arvanov A N, Gavalyan V G, Lorikyan M P, Preprint EFM-195(39) (Erevan: 1981)
41. Arvanov A N, Gavalyan V G, Lorikyan M P *Prib. Tekh. Eksp.* (4) 70 (1983)
42. Kavalov R L, Luk'yanov S M, Markaryan Yu L, et al., Preprint OIYaI 13-83-188 (Dubna: Joint Institute of Nuclear Research, 1983); *Prib. Tekh. Eksp.* (3) 45 (1984)
43. Kavalov R L, Markaryan Yu L, Panyan M G, Panyan G A, Preprint EFI-673(63) (Erevan: 1983)
44. Kavalov R L, Luk'yanov S M, Markaryan Yu L, et al. *Prib. Tekh. Eksp.* (3) 42 (1985)
45. Chianelli C, Ageron P, Bouvet J P, et al. *Nucl. Instrum. Methods Phys. Res. A* **273** 245 (1988)
46. Gukasyan S M, Alanakyan A K, Martirosyan E S *Izv. Akad. Nauk Arm. SSR Fiz.* **24** 203 (1989)
47. Gavalyan V G, Lorikyan M P, Arvanov A N *Izv. Akad. Nauk Arm. SSR Fiz.* **17** 102 (1982)
48. Kharitonov V M, Preprint EFI-248(41) (Erevan: 1977)
49. Gavalyan V G, Preprint EFI-1238(24) (Erevan: 1990)
50. Arvanov A N, Akhperdzhanyan A G, Gavalyan V G, et al. *Radiotekh. Elektron.* **27** 163 (1982)
51. Busch F, Pfeffer W, Kohlmeyer B, et al. *Nucl. Instrum. Methods* **171** 71 (1980)
52. Gukasian S M, Kavalov R L, Lorikian M P, Trofimchuk N N, Preprint EPI-280(5) (Erevan: 1978)
53. Gukasyan S M, Kavalov R L, Lorikyan M P, et al., Preprint EFI-370(28) (Erevan: 1979)
54. Gukasyan S M, Kavalov R L, Lorikyan M P, Preprint EFI-372(30) (Erevan: 1979)
55. Gukasyan S M, Kavalov R L, Lorikyan M P, Petrosyan G G *Izv. Akad. Nauk Arm. SSR Fiz.* **44** 634 (1980)
56. Gukasian S M, Kavalov R L, Lorikian M P, Markarian Yu L *Nucl. Instrum. Methods* **167** 427 (1979)
57. Gukasian S M, Kavalov R L, Lorikian M P *Nucl. Instrum. Methods* **171** 469 (1980)
58. Frenkel I Ya *Z. Phys.* **35** 652 (1926); Gukasyan S M, Kavalov R L, Lorikyan M P, Author's Certificate No. 824 808 (1982), in *Byull. Izobret.* (20) 200 (1982)
59. Lorikyan M P, Markaryan K Zh, Tarlamazyan B G *Prib. Tekh. Eksp.* (5) 45 (1984)
60. Lorikyan M P, Gavalyan V G, Gukasyan S M, et al. *Tr. II Mezhdunar. Simpoziuma po Perekhodnomu Izlucheniyu Chastits Vysokikh Energii, Erevan, 1983* (Proceedings of Second International Symposium on Transition Radiation of High-Energy Particles, Erevan, 1983) (Erevan: Erevan Physics Institute, 1984) p. 648
61. Gavalian V G, Lorikian M P, Markarian K J *Nucl. Instrum. Methods Phys. Res. A* **350** 244 (1994)
62. Gavalyan V G, Arvanov A N, Lorikyan M P, Gukasyan S M *Prib. Tekh. Eksp.* (4) 72 (1984)
63. Gavalyan V G, Lorikyan M P, Gukasyan S M *Tr. II Mezhdunarodnogo Simpoziuma po Perekhodnomu Izlucheniyu Chastits Vysokikh Energii, Erevan, 1993* (Proceedings of Second Symposium on Transition Radiation of High-Energy Particles, Erevan, 1993) (Erevan: Erevan Physics Institute, 1994) p. 640
64. Mkrtchyan A R, Gukasyan S M, Kocharyan L A *Izv. Akad. Nauk Arm. SSR Fiz.* **24** 198 (1989)
65. Lorikian M P, Gavalian V G *Nucl. Instrum. Methods Phys. Res. A* **340** 625 (1994)
66. Avakyan R O, Gavalyan V G, Lorikyan M P, et al., Preprint EFI-1164(41) (Erevan: 1989); *Vopr. At. Nauki Tekh. Ser. Yad. Fiz. Issled.* (3/11) (1990)
67. Gavalyan V G, Lorikyan M P, Sarkisyan Yu G, Preprint EFI-813(40) (Erevan: 1985)
68. Gavalian V G, Lorikian M P, Shikhliarov K K *Nucl. Instrum. Methods Phys. Res. A* **337** 613 (1994)
69. Lukasyan S M, Preprint EFI-640(30) (Erevan: 1983)
70. Lorikian M P (in press)